ISTITUTO NAZIONALE DI RICERCA METROLOGICA
Repository Istituzionale

A correction method for Vickers indenters squareness measurement due to the tilt of the pyramid axis

This is the author's submitted version of the contribution published as:

Original
A correction method for Vickers indenters squareness measurement due to the tilt of the pyramid axis / Prato, Andrea; Galliani, Davide; Origlia, Claudio; Germak, ALESSANDRO FRANCO LIDIA. - In: MEASUREMENT. - ISSN 1536-6367. - 140:(2019), pp. 565-571. [10.1016/j.measurement.2019.04.007]

Availability:
This version is available at: 11696/60574 since: 2021-04-13T15:09:30Z

Publisher:
Elsevier

Published
DOI:10.1016/j.measurement.2019.04.007

Terms of use:

This article is made available under terms and conditions as specified in the corresponding bibliographic description in the repository

Publisher copyright

(Article begins on next page)

03 May 2024

A correction method for Vickers indenters squareness measurement due to the tilt of the pyramid axis

Andrea Prato[1], Davide Galliani[2], Claudio Origlia[1] and Alessandro Germak[1]

[1] *INRiM - Istituto Nazionale di Ricerca Metrologica, 10135 Torino, Italy*
[2] *LTF S.p.A. - 24051 Antegnate (BG), Italy*

Corresponding author e-mail: *a.prato@inrim.it*

Abbreviated title: Vickers indenter squareness measurement correction

Abstract

In ISO 6507-3 it is required that the quadrilateral base of Vickers indenter has angles of 90° ± 0.2°. Squareness angles are usually evaluated through optical techniques by measuring the angles between two consecutive faces, which correspond to the quadrilateral base angles when the axis of the pyramid is perfectly parallel to the indenter-holder axis. However, if the pyramid axis is tilted by an angle within 0.3°, as allowed by the standard, these angles no longer correspond. This work deals with the description of a numerical method, based on a proper geometrical model, to correct squareness measurements. The proposed method is applied to experimental tests and measurement results, with related uncertainties, are presented. It is shown that the accuracy is improved. This method is easily implementable on different measuring systems and can be internationally adopted to improve the relevant standard.

Keywords: Hardness, Vickers indenter, squareness.

1. Introduction

The influence of indenter characteristics on hardness measurements, in particular for Vickers hardness, is largely reported in literature. It has been demonstrated that different indenters meeting the requirements of the Standards can lead to significantly different hardness measurements, and in particular that an increase in indenter angle entails a decrease in Vickers hardness [1,2]. It was also found that squareness errors and ridge, within the required tolerances, entail small errors in Vickers hardness [3], beyond the influence of the optical system for the evaluation of the indentation impression [4]. Also in Rockwell hardness, it was found that the main causes of differences in performance are due to imperfections in the geometric form of the indenter [5,6], and in particular that an increasing angle of the indenter entails an increase in hardness value [7]. Other works showed that hardness measurements can be affected by the roughness or mechanical deformations of the indenter under load [8] or by form errors of the indenter [9], in Rockwell C, or by friction between the indenter and material for Berkovich and cubic indenters, in microindentation hardness [10].

ISO 6507-3 [11] specifies the requirements of the diamond pyramidal indenter used for the calibration of hardness reference blocks. They are composed of a highly polished square-based diamond pyramid with an angle between the opposite faces of the vertex of 136° ± 0.1°, placed upon a steel indenter-holder, as shown in Fig. 1.

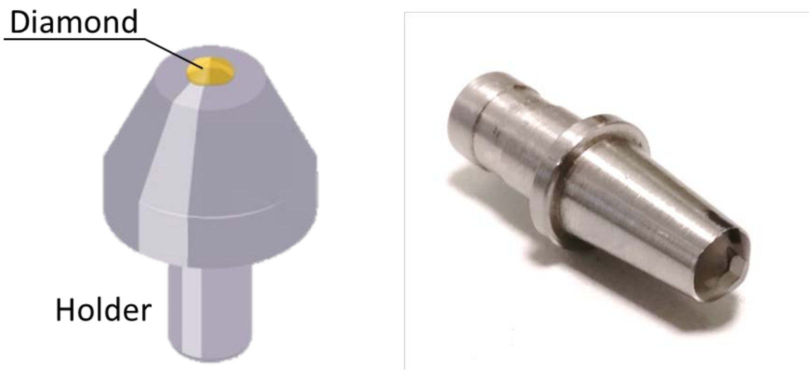

Fig. 1. 3-D model (left) and picture (right) of a typical Vickers indenter.

The pyramid quadrilateral base, which is given by the intersection of the faces with a plane perpendicular to the axis of the diamond pyramid, should have angles of 90° ± 0.2°. These angles are usually evaluated by measuring the angles $\gamma_{\exp,i=1,2,3,4}$ between two consecutive faces, assuming the indenter-holder axis as reference [12,13]. Furthermore, the angle between the pyramid axis and the indenter-holder axis (normal to the seating surface), which represents the tilt angle of the pyramid axis, should be less than 0.3°. Nevertheless, the effect of this tilt on the measurement of the quadrilateral base angles, namely squareness measurement, is not considered in the current international standard. As a matter of fact, when the pyramid axis and indenter-holder axis, normal to the seating surface, are not parallel, the angles $\gamma_{\exp,i}$ between two consecutive faces are different from the quadrilateral base angles $\varphi_{i=1,2,3,4}$. Such behavior affects the accuracy of squareness measurement, thus a correction is needed. In this work, a correction method, derived from a proper geometrical model, is proposed and described in the following Sections.

2. Measurement of Vickers indenters geometry

ISO 6507-3 (Sec. 5.5) requires that the indenter meets some geometrical requirements [11]. These measurements are usually performed in calibration laboratories by means of optical measuring systems [12-20]. In particular, the measurement of the four quadrilateral base angles φ_i is performed with microscopes that use angular encoders [21] or with scanning confocal chromatic probes [13]. Both methods use the indenter-holder axis or seating holder as reference. In this condition, measured angles $\gamma_{\exp,i}$ correspond to the actual quadrilateral base angles φ_i when the axis of the pyramid is parallel to the indenter-holder axis, i.e. when it is perpendicular to the seating surface plane. However, these angles are not the same when the pyramid axis is tilted by an angle β, as shown in Fig. 2.

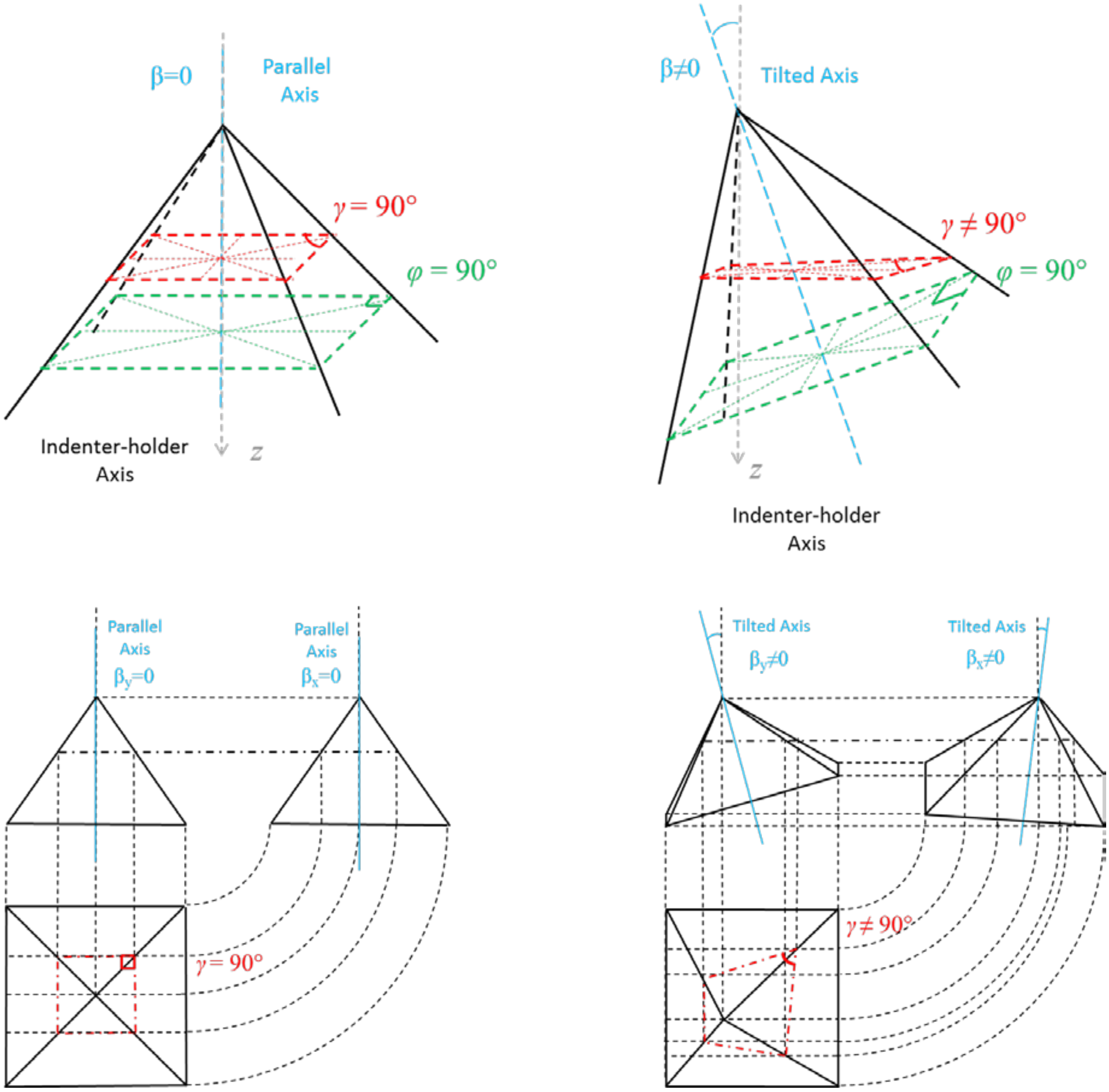

Fig. 2. Representation of a generic pyramid with a parallel axis (left) and a tilted axis (right) with respect to the indenter-holder axis, in cabinet perspective (top) and in orthogonal projection (bottom). The actual square-base angles are depicted in green and the measured angles between two consecutive faces are depicted in red.

By way of example, in INRiM hardness laboratory, the Galileo-LTF® Gal-Indent optical system is adopted (Fig. 3) [12]. This system is able to measure the two vertex angles α_x and α_y of the indenter (nominally 136°) along *x*- and *y*- axis, respectively, between two opposite faces, and the four angles $\gamma_{\exp,i}$ between two consecutive faces (nominally 90°) by means of two angular encoders mounted on the optical measuring system [21].

Fig. 3. The Galileo-LTF® Gal-Indent optical system used at INRiM hardness laboratory for the measurement of the vertex angles and the quadrilateral base angles.

Its geometrical characteristics assure that all mechanical parts are perfectly aligned and that the Vickers indenter-holder axis is perpendicular to the lens of the system. The optical system is based on Mirau interferometry, where a light beam (wavelength of 546 nm) is split into two beams: one is reflected to the observer (either through the eyepieces or through a TV Camera), the other hits a Vickers indenter lateral face and is reflected to the observer as well. The two beams recombine and generate an interference pattern. The indenter is simultaneously rotated around the axis passing through the pyramid vertex normal to the plane containing the indenter-holder axis and the optical lens axis, and around the indenter-holder axis, until a lateral face is parallel to the plane of the microscope lens by observing the interference fringes. These two rotations are measured by means of two angular encoders. Rotations around the indenter-holder axis represent the measurement of the angles $\gamma_{\exp,i}$ between two consecutive faces, whereas, for each lateral face, rotations around the axis passing through the pyramid vertex normal to the plane containing the indenter-holder axis and the optical lens axis represent the measurement of the supplementary angles (ω_{x-}, ω_{x+}, ω_{y-}, ω_{y+}) along *x*- and *y*-axis in clockwise (-) and counter clockwise (+) directions, according to Fig. 4. In this way, the two vertex angles α_x and α_y and the pyramid tilt angles β_x and β_y, along *x*- and *y*- axis, can be calculated, respectively, according to to Eqs. (1) and Eqs. (2). By way of example, in Fig. 4, the cross-section of a Vickers indenter through *yz* plane shows the measured vertex angle α_y and the tilt angle β_y.

By decomposing the pyramid tilted axis vector **v** along *xz* and *yz* planes, according to Fig. 5, Eq. (3) and Eq. (4) can be derived and combined. From Eq. (4), it is then possible to derive the relationship between the total tilt angle β and the pyramid tilt angles β_x and β_y, along *x*- and *y*- axis, as shown in Eq. (5), which, in turn, can be approximated to Eq. (6) by applying small-angle approximation as the angle between the pyramid axis and the indenter-holder axis is in the order of 10^{-1} °.

$$\alpha_x = 180 - (\omega_{x+} + \omega_{x-}); \qquad \alpha_y = 180 - \left(\omega_{y+} + \omega_{y-}\right) \tag{1}$$

$$\beta_x = \frac{\omega_{x+} - \omega_{x-}}{2}; \quad \beta_y = \frac{\omega_{y+} - \omega_{y-}}{2} \tag{2}$$

$$\|\mathbf{v}\| \cos\beta = \|\mathbf{v}_{xz}\| \cos\beta_x = \left\|\mathbf{v}_{yz}\right\| \cos\beta_y \tag{3}$$

$$\begin{aligned} \|\mathbf{v}\| \sin\beta &= \sqrt{(\|\mathbf{v}_{xz}\| \sin\beta_x)^2 + \left(\left\|\mathbf{v}_{yz}\right\| \sin\beta_y\right)^2} = \\ &= \sqrt{\left(\frac{\|\mathbf{v}\| \cos\beta}{\cos\beta_x} \sin\beta_x\right)^2 + \left(\frac{\|\mathbf{v}\| \cos\beta}{\cos\beta_y} \sin\beta_y\right)^2} = \|\mathbf{v}\| \cos\beta \sqrt{\left(\frac{\sin\beta_x}{\cos\beta_x}\right)^2 + \left(\frac{\sin\beta_y}{\cos\beta_y}\right)^2} \end{aligned} \tag{4}$$

$$\tan\beta = \sqrt{(\tan\beta_x)^2 + (\tan\beta_y)^2} \tag{5}$$

$$\beta = \sqrt{{\beta_x}^2 + {\beta_y}^2} \tag{6}$$

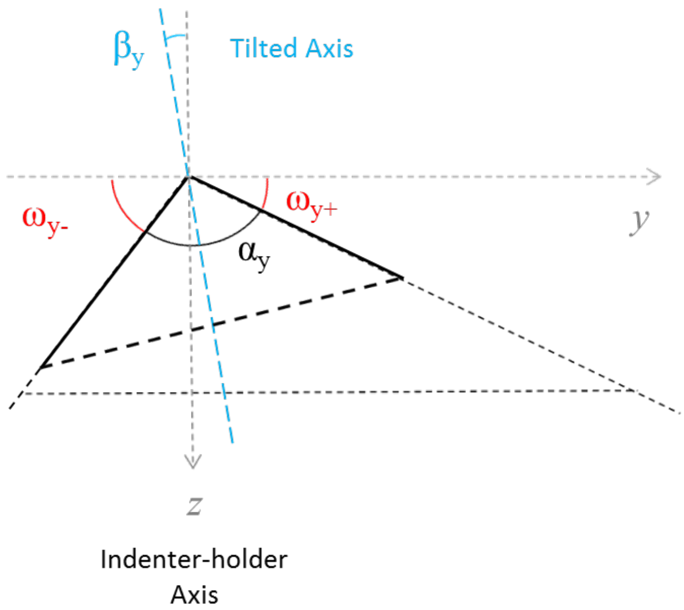

Fig. 4. Cross-section of Vickers indenter angles measured with the optical system through *yz* plane.

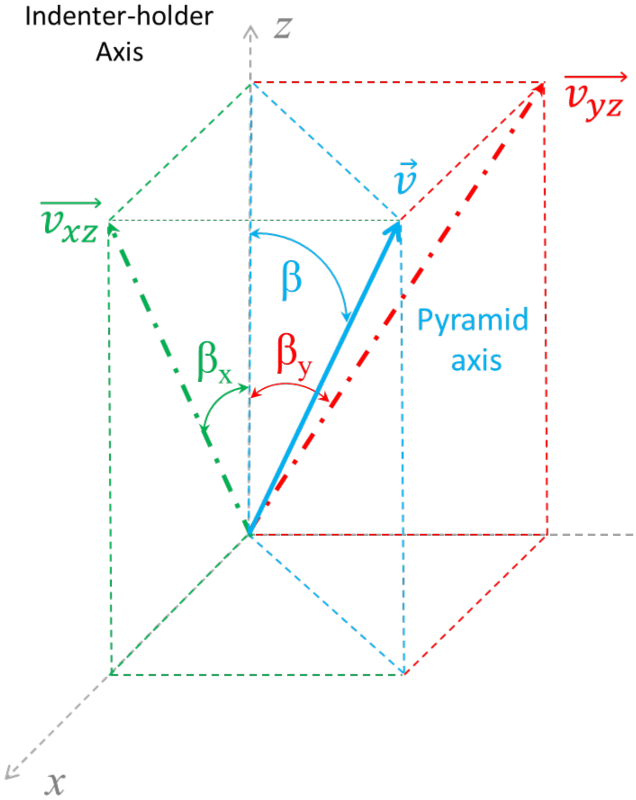

Fig. 5. Decomposition of the tilted pyramid axis vector **v** and the associated angles along *x*- and *y*- axis.

3. Correction method

The geometrical model at the base of the correction method aims to calculate the theoretical angles γ_i of an ideal square-based pyramid with a tilted axis with respect to the indenter-holder axis, and correct the measured quadrilateral base angles $\gamma_{\exp,i}$. The following equations are based on fundamental elements of linear algebra [22].

Firstly, by cutting the tilted pyramid with a horizontal plane (z = 1) perpendicular to the indenter-holder axis unit vector **k** = (0,0,1), the vectors **v'** and $\mathbf{p}_{i=1,2,3,4}$, which represent the vectors of the bisector between the indenter-holder axis **k** and the pyramid axis **v**, and the four lateral edges of the associated right pyramid, respectively, are defined according to Eqs. (7). Vectors are shown in Fig. 6 (left) and Fig. 7 (top-left). The bisector between the indenter-holder axis **k** and the pyramid axis **v** is used to perform the rotation of the lateral edge vectors $\mathbf{p}_i$ by finding its symmetrical vectors $\mathbf{q}_i$, as described below.

$$\begin{cases} \mathbf{v}' = (v'_x, v'_y, v'_z) = \left(\tan\frac{\beta_x}{2}, \tan\frac{\beta_y}{2}, 1\right) \\ \mathbf{p_1} = (p_{1x}, p_{1y}, p_{1z}) = \left(\tan\frac{\alpha_x}{2}, -\tan\frac{\alpha_y}{2}, 1\right) \\ \mathbf{p_2} = (p_{2x}, p_{2y}, p_{2z}) = \left(\tan\frac{\alpha_x}{2}, \tan\frac{\alpha_y}{2}, 1\right) \\ \mathbf{p_3} = (p_{3x}, p_{3y}, p_{3z}) = \left(-\tan\frac{\alpha_x}{2}, \tan\frac{\alpha_y}{2}, 1\right) \\ \mathbf{p_4} = (p_{4x}, p_{4y}, p_{4z}) = \left(-\tan\frac{\alpha_x}{2}, -\tan\frac{\alpha_y}{2}, 1\right) \end{cases} \tag{7}$$

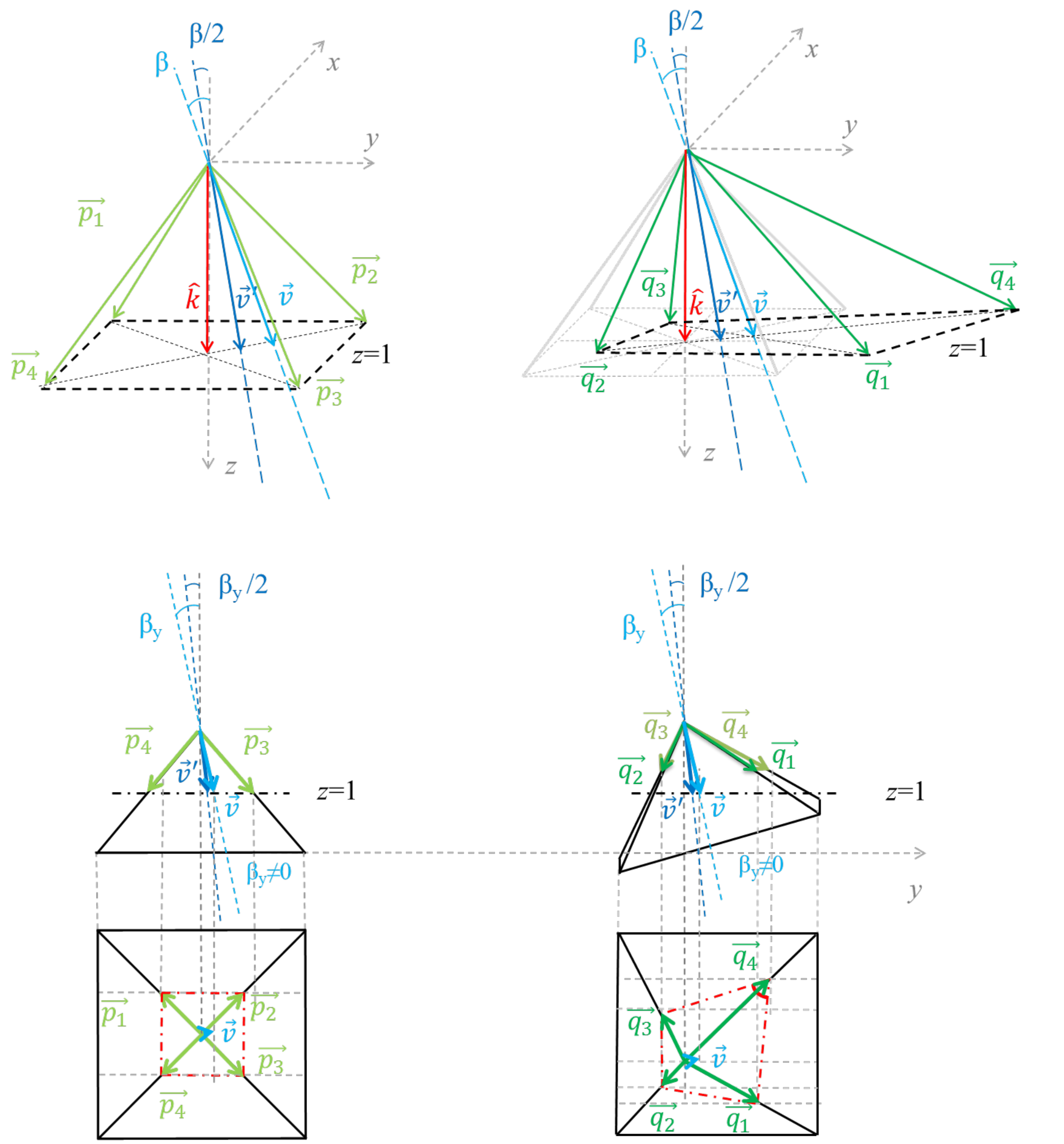

Fig. 6. Vectors of the associated right pyramid (left) and the tilted pyramid (right) in cabinet perspective (top) and in orthogonal projection (bottom).

By tilting the pyramid by an angle β, the vectors $\mathbf{p}_{\mathbf{v'},\mathbf{i}}$, which represent the projection of $\mathbf{p}_\mathbf{i}$ on **v'**, can be defined according to Eq. (8) and are shown in Fig. 7 (top-right).

$$\mathbf{p}_{\mathbf{v}',\mathbf{i}} = \left(\mathrm{p}_{\mathrm{v}',\mathrm{ix}}, \mathrm{p}_{\mathrm{v}',\mathrm{iy}}, \mathrm{p}_{\mathrm{v}',\mathrm{iz}}\right) = \tag{8}$$

$$= \left(\left(\mathbf{p_i} \cdot \frac{\mathbf{v}'}{\|\mathbf{v}'\|} \right) \frac{\mathrm{v}'_x}{\|\mathbf{v}'\|}, \left(\mathbf{p_i} \cdot \frac{\mathbf{v}'}{\|\mathbf{v}'\|} \right) \frac{\mathrm{v}'_y}{\|\mathbf{v}'\|}, \left(\mathbf{p_i} \cdot \frac{\mathbf{v}'}{\|\mathbf{v}'\|} \right) \frac{\mathrm{v}'_z}{\|\mathbf{v}'\|} \right)$$

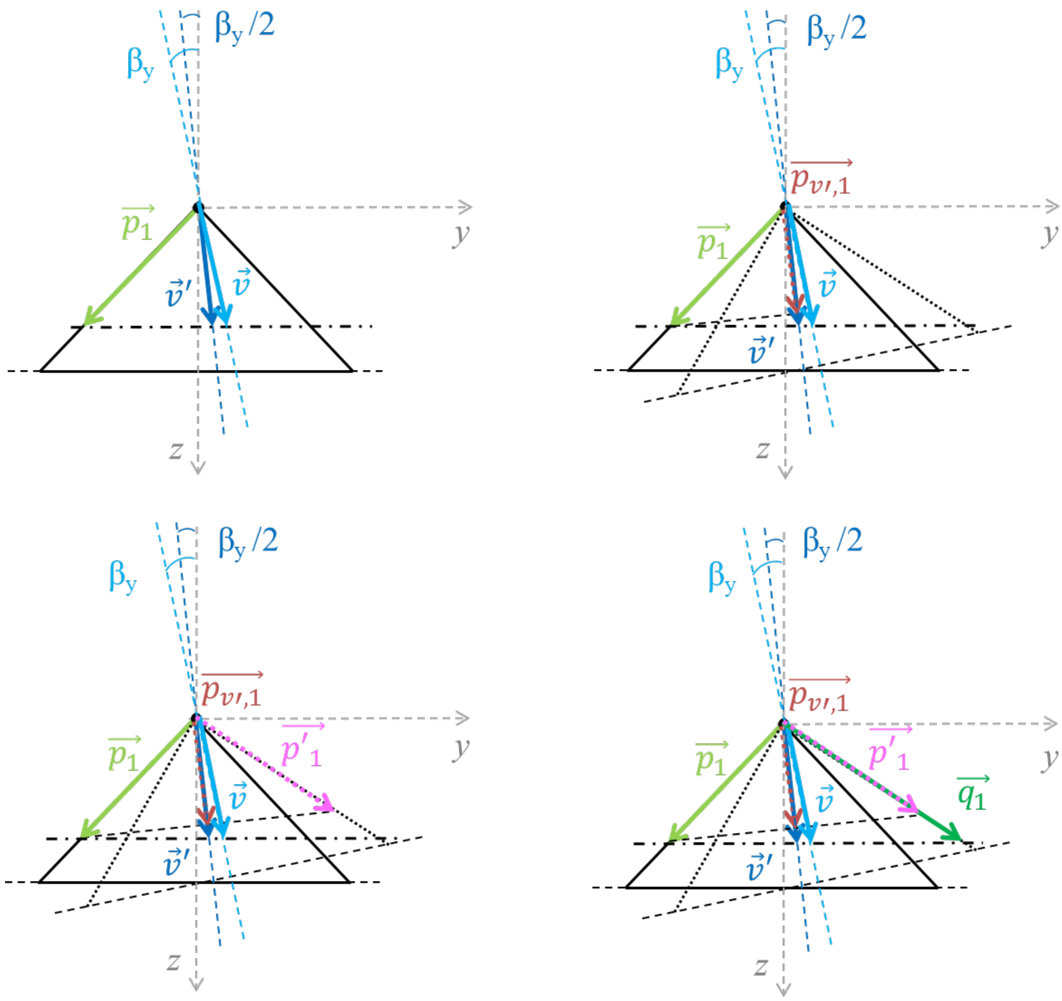

Fig. 7. Defined vectors (for *i*=1) on the *yz* plane cross-section.

Considering the tip of vector $\mathbf{p}_{\mathbf{v'},\mathbf{i}}$ as the midpoint, it is possible to get the lateral edge vectors $\mathbf{p'_i}$ symmetrical to $\mathbf{p_i}$, according to Eq. (9), as depicted in Fig. 7 (bottom-left).

$$\mathbf{p}'_\mathbf{i} = (\mathrm{p'}_{ix}, \mathrm{p'}_{iy}, \mathrm{p'}_{iz}) = (2\mathrm{p}_{v',ix} - \mathrm{p}_{ix}, 2\mathrm{p}_{v',iy} - \mathrm{p}_{iy}, 2\mathrm{p}_{v',iz} - \mathrm{p}_{iz}) =$$
$$= \left(2\left(\mathbf{p_i} \cdot \frac{\mathbf{v}'}{\|\mathbf{v}'\|} \right) \frac{\mathrm{v}'_x}{\|\mathbf{v}'\|} - \mathrm{p}_{ix}, 2\left(\mathbf{p_i} \cdot \frac{\mathbf{v}'}{\|\mathbf{v}'\|} \right) \frac{\mathrm{v}'_y}{\|\mathbf{v}'\|} - \mathrm{p}_{iy}, 2\left(\mathbf{p_i} \cdot \frac{\mathbf{v}'}{\|\mathbf{v}'\|} \right) \frac{\mathrm{v}'_z}{\|\mathbf{v}'\|} - \mathrm{p}_{iz} \right) \quad (9)$$

Then, by stretching the vectors **p'**$_\mathbf{i}$ to the plane z=1 and reminding that p_{iz}=1, it is possible to obtain the vectors $\mathbf{q_i}$, which represent the lateral edge vectors of the tilted square-base pyramid, according to Eq. (10). These vectors are represented in Fig. 6 (right) and Fig.7 (bottom-right).

$$\mathbf{q_i} = (\mathrm{q_{ix}}, \mathrm{q_{iy}}, \mathrm{q_{iz}}) = \left(\frac{2\left(\mathbf{p_i} \cdot \frac{\mathbf{v}'}{\|\mathbf{v}'\|}\right)\frac{\mathrm{v}'_x}{\|\mathbf{v}'\|} - \mathrm{p_{ix}}}{2\left(\mathbf{p_i} \cdot \frac{\mathbf{v}'}{\|\mathbf{v}'\|}\right)\frac{\mathrm{v}'_z}{\|\mathbf{v}'\|} - \mathrm{p_{iz}}}, \frac{2\left(\mathbf{p_i} \cdot \frac{\mathbf{v}'}{\|\mathbf{v}'\|}\right)\frac{\mathrm{v}'_y}{\|\mathbf{v}'\|} - \mathrm{p_{iy}}}{2\left(\mathbf{p_i} \cdot \frac{\mathrm{v}'_z}{\|\mathbf{v}'\|}\right)\frac{\mathrm{v}'_z}{\|\mathbf{v}'\|} - \mathrm{p_{iz}}}, 1 \right) =$$
$$= \left(\frac{2(\mathbf{p_i} \cdot \mathbf{v}')\mathrm{v}'_x - \mathrm{p_{ix}}\|\mathbf{v}\|^2}{2(\mathbf{p_i} \cdot \mathbf{v}')\mathrm{v}'_z - \mathrm{p_{iz}}\|\mathbf{v}\|^2}, \frac{2(\mathbf{p_i} \cdot \mathbf{v}')\mathrm{v}'_y - \mathrm{p_{iy}}\|\mathbf{v}'\|^2}{2(\mathbf{p_i} \cdot \mathbf{v}')\mathrm{v}'_z - \mathrm{p_{iz}}\|\mathbf{v}'\|^2}, 1 \right) = \tag{10}$$
$$= \left(\frac{2(\mathbf{p_i} \cdot \mathbf{v}')\mathrm{v}'_x - \mathrm{p_{ix}}\|\mathbf{v}'\|^2}{2(\mathbf{p_i} \cdot \mathbf{v}') - \|\mathbf{v}'\|^2}, \frac{2(\mathbf{p_i} \cdot \mathbf{v}')\mathrm{v}'_y - \mathrm{p_{iy}}\|\mathbf{v}'\|^2}{2(\mathbf{p_i} \cdot \mathbf{v}') - \|\mathbf{v}'\|^2}, 1 \right)$$

By subtracting two consecutive vectors $\mathbf{q_i}$, the quadrilateral base vectors $\mathbf{r_i}$ are obtained according to Eqs. (11), and the theoretical angles γ_i of a tilted square-based pyramid can thus be found according to Eqs. (12) (see Fig. 8).

$$\begin{cases} \mathbf{r_{i=1,2,3}} = \mathbf{q_i} - \mathbf{q_{i+1}} \\ \mathbf{r_4} = \mathbf{q_4} - \mathbf{q_1} \end{cases} \tag{11}$$

$$\begin{cases} \gamma_{i=1,2,3} = \cos^{-1}\left(\frac{\mathbf{r_i} \cdot (-\mathbf{r_{i+1}})}{\|\mathbf{r_i}\| \cdot \|\mathbf{r_{i+1}}\|} \right) \\ \gamma_4 = 360 - \gamma_1 - \gamma_2 - \gamma_3 \end{cases} \tag{12}$$

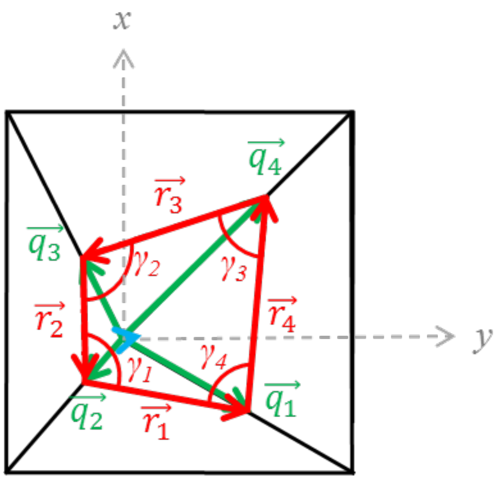

Fig. 8. Quadrilateral base vectors and angles.

In this way, the measured angles $\gamma_{\text{exp},i}$ can be corrected and the actual angles φ_i of the quadrilateral base of the tilted pyramid can be numerically evaluated according to Eq. (13).

$$\varphi_i = 90 + \gamma_{exp,i} - \gamma_i \tag{13}$$

4. Measurement results and associated uncertainty

In this Section, the application of the numerical correction method to experimental squareness measurements is presented. The Vickers indenter under test is a Galileo-LTF® indenter. Measurements are performed at INRiM with the Galileo-LTF® Gal-Indent optical system, described in Section 2. Currently, at international level, traceability of Vickers diamond indenter angle measurements, according to ISO 6507-3, are guaranteed by INRiM with absolute expanded uncertainties (k = 2, 95 % of confidence level) of 0.05° for the tilt angle β, for the angles between the opposite faces of the vertex α and for the angles of the quadrilateral base $\gamma_{\text{exp},i}$.

In this illustrative case, the measured supplementary angles of the diamond pyramidal indenter along x- and y- directions (ω_{x+}, ω_{x-}, ω_{y+}, ω_{y-}) are 21.980°, 22.089°, 22.131° and 21.955°, respectively, and the measured squareness angles between two consecutive faces ($\gamma_{\text{exp},1}$, $\gamma_{\text{exp},2}$, $\gamma_{\text{exp},3}$, $\gamma_{\text{exp},4}$) are 90.11°, 90.38°, 89.95° and 89.57°, respectively. According to Eq. (1), the measured vertex angles α_x and α_y of the indenter along x-

and y-axis are 135.93° and 135.91°, respectively. Both are within the corresponding tolerance interval (136° ± 0.1°). The tilt angles β_x and β_y, evaluated according to Eq. (2), are -0.05° and 0.09°, respectively, thus the total tilt angle is 0.10°, according to Eq. (6), which is within the standard tolerance of 0.30°. These data are used as inputs in the previous equations and, in this way, the theoretical angles of the associated square-base pyramid γ_i can be found.

Squareness angles $\gamma_{\mathrm{exp},i}$, theoretical angles of the associated tilted square-base pyramid γ_i, and the corrected angles φ_i, according to Eq. (13), along with the expanded uncertainties (coverage factor, k=2) evaluated according to GUM [23], are listed in Table 1.

It is observed that without the correction, two angles (2 and 4) are outside the tolerance interval. The difference between corrected and measured angles (φ_i-$\gamma_{exp,i}$) to show the magnitude of correction, and the difference between corrected angles φ_i and 90° to verify the compliance with the requirement of the relevant standard, are also reported. It is shown that the maximum correction is 0.35° and that the application of the proposed procedure allows, in this illustrative case, to fulfill the standard requirements.

Table 1

Experimental squareness measurement with the implementation of the correction method.

Angle i	Measured angle $\gamma_{\mathrm{exp},i}$ / °	Theoretical angle γ_i / °	Corrected angle φ_i / °	φ_i - $\gamma_{exp,i}$ / °	φ_i - 90 / °
1	90.11 ± 0.05	90.10 ± 0.03	90.01 ± 0.06	-0.10 ± 0.06	0.01 ± 0.06
2	90.38 ± 0.05	90.34 ± 0.03	90.04 ± 0.06	-0.34 ± 0.06	0.04 ± 0.06
3	89.95 ± 0.05	89.90 ± 0.03	90.05 ± 0.06	0.10 ± 0.06	0.05 ± 0.06
4	89.57 ± 0.05	89.65 ± 0.03	89.92 ± 0.06	0.35 ± 0.06	-0.08 ± 0.06

5. Conclusions

ISO 6507-3 specifies that the quadrilateral base of the diamond pyramidal Vickers indenter used for the calibration of hardness reference blocks has angles of 90° ± 0.2°. This measurement is usually performed with optical techniques by measuring the angles between two consecutive lateral faces, using the indenter-holder axis or seating holder as reference. However, if the pyramid axis is tilted by a maximum angle of 0.3° with respect to the indenter-holder axis, as allowed by the standard, squareness measurement is not accurate enough. In fact, in this case, the actual quadrilateral base angles do not correspond to the angles between two consecutive faces. Such behavior affects the accuracy of squareness measurement, thus a correction is needed. In this work, a numerical correction method, derived from a proper geometrical model of the Vickers indenter, is finally proposed and described to overcome this issue. Its implementation on experimental measurements, reported along with the associated uncertainties, shows that the correction method improves the accuracy of Vickers indenters squareness measurement. Furthermore, since it is suitable for different measuring systems and is easily implementable, even on common spreadsheets, the method can be adopted internationally, in the future, to improve the relevant standard. Future works will be aimed at extending the correction method for Rockwell and Berkovich indenters and at evaluating more in-depth the direct influence of squareness and tilt errors on Vickers hardness tests.

Acknowledgment

The authors are thankful to Galliani Valerio and Turotti Francesco from LTF S.p.A. (Antegnate, Italy) for supporting the work and providing precious and essential suggestions.

References

[1] L. Brice, The influence of indenter characteristics on hardness measurements, in: Proceedings of XVII IMEKO World Congress Metrology, Dubrovnik, Croatia, June 22-27, 2003.

[2] M. El-Sherbiny, R. Hegazy, M. Ibrahim, and A. Abuelezz, The influence of geometrical tolerances of Vickers indenter on the accuracy of measured hardness, Int. J. Metrol. Qual. Eng. 3 (2012) 1–6.

[3] F. Petik, Factors influencing hardness measurement (a systematic survey of research results), Bureau International de Metrologie Legale, Paris, (1983).

[4] G. Barbato, S. Desogus, Problems in the measurement of Vickers and Brinell indentations, Measurement 4(4) (1986) 137-147.

[5] G. Barbato, F. Petik, Metrological involvement in the definition and dissemination of hardness scales, in: Proceedings of XIII IMEKO, vol. 1, Torino, 1994, pp. 761–766.

[6] R.S. Marriner, J.G. Wood, Investigation into the measurement and performance of Rockwell C diamond indenters, Metallurgia 87 (1967) 87–90.

[7] G. Barbato, S. Desogus, R. Levi, The meaning of the geometry of Rockwell indenters, IMGC Tech. Rep. R128 (1978).

[8] G. Barbato, M. Galetto, A. Germak, F. Mazzoleni, Influence of the indenter shape in Rockwell hardness test, in: Proceedings of the HARDMEKO '98, September 21–23, Beijing, China, 1998, pp. 53–60.

[9] J. Song, S. Low, L. Ma, Form error and hardness performance of Rockwell diamond indenters, in: Proceedings of 16th World Congress of International Measurement Confederation (IMEKO XVI), Vienna, Austria, September 01, 2000, p. 6.

[10] J. Qin, Y. Huang, K.C. Hwang, J. Song, G.M. Pharr, The effect of indenter angle on the microindentation hardness, Acta Materialia 55 (2007) 6127–6132.

[11] ISO 6507-3:2018 Metallic materials - Vickers hardness test - Part 3: Calibration of reference blocks.

[12] A. Liguori, A. Germak, G. Gori, E. Messina, Galindent: the reference metrological system for the verification of the geometrical characteristics of Rockwell and Vickers diamond indenters, In: VDI/VDE-GMA, IMEKO TC3/TC5/TC20 Joint International Conference, 24-26 Sept. 2002, VDI-Berichte 1685, Tagung Celle, Germany, 2002, pp. 365-371.

[13] T. Sanponpute, W. Limthunyalak, F. Menelao, D. Schwenk, Vickers indenter shape measurement by using scanning confocal chromatic instrument, in: Proceedings of XXI IMEKO World Congress "Measurement in Research and Industry", Prague, Czech Republic, August 30 - September 4, 2015.

[14] R. Affri, S. Desogus, A. Germak, F. Mazzoleni, D. Perteghella, Optical measuring system for hardness indenters, in: Proceedings of XVI IMEKO World Congress Measurement, Vienna, Austria, September 25-28, 2000.

[15] S. Takagi, K. Kamijo, T. Usuda, H. Kawachi, K. Hanaki, Wide-range verification of the geometry of Vickers diamond indenters, in: Proceedings of XVIII IMEKO World Congress Measurement, Rio de Janeiro, Brazil, September 17-22, 2006.

[16] S. Takagi, T. Ishibashi, Analysis of indenter geometry verification data by means of the regression plane fitting, in: Proceedings of IMEKO 2010 TC3, TC5 and TC22 Conferences Metrology in Modern Context, Pattaya, Chonburi, Thailand, November 22–25, 2010.

[17] K. Hasche, K. Herrmann, F. Pohlenz, K. Thiele, Determination of the geometry of microhardness indenters with a scanning force microscope, Meas. Sci. Technol. 9 (1998) 1082–1086.

[18] A. Germak, K. Herrmann, G. Dai, Z. Li, Development of calibration methods for hardness indenters, VDI-Berichte 1948, 2006, pp. 13–26..

[19] L. Zhang, Y. Cui, F. Zhang, Optical measuring system for the geometrical parameters of Rockwell and Vickers diamond hardness indenters, in: Proceedings of LIDAR Imaging Detection and Target Recognition Volume 10605, Changchun, China, 23-25 July, 2017.

[20] A. Germak, C. Origlia, Investigations of new possibilities in the calibration of diamond hardness indenters geometry, Measurement 44 (2011) 351–358.

[21] A. Germak, A. Liguori, C. Origlia, Experience in the metrological characterization of primary hardness standard machines, in: Proceedings of HARDMEKO 2007, Tsukuba, Japan, November 19-21, 2007, pp. 81-89.

[22] S. Lipschutz, M.L. Lipson, Linear Algebra, fifth ed., Mc Graw Hill, New York, 2009.

[23] JCGM 100:2008, Evaluation of Measurement Data — Guide to the Expression of Uncertainty in Measurement (GUM), Joint Committee for Guides in Metrology, Sèvres, France.